EPS-0483
Submitted to Pa 10,17 and Pl 1,2,3

Charged Particle Multiplicities in Deep-Inelastic Scattering at HERA

H1 Collaboration

Abstract

Using the H1 detector at HERA, the charged particle multiplicity distributions in deep-inelastic ep scattering have been measured over a large kinematical region. The evolution with W and Q^2 of the average charged hadron multiplicity $\langle n_{ch} \rangle$ and the ratio of $\langle n_{ch} \rangle$ to the dispersion D of the multiplicity distributions is studied in the current fragmentation region of the hadronic CMS frame. The results are compared to lower-energy lepton-nucleon data and to e^+e^- annihilation results.

1 Introduction

In this paper we present preliminary results on a study of the multiplicity distribution (MD) of charged hadrons produced in deep-inelastic scattering (DIS) e^+p collisions at HERA. The analysis is based on data accumulated in 1994. Analyses of the multiplicity distribution in the Breit-frame at HERA can be found in [1, 2].

The multiplicity distribution of charged hadrons is one of the basic observables characterising multiparticle final states in high-energy interactions. Data are available for the full variety of collision processes from e^+e^- annihilations to nucleus-nucleus collisions, and span a wide range of energies [3, 4]. On the theoretical and phenomenological side, numerous studies were devoted to the subject [5–7], starting with early investigations by Heisenberg [8] and Fermi [9].

A proper description of the hadron multiplicity, and of its fluctuations, in a high-energy collision requires detailed understanding of the hadronisation mechanism and confinement in quantum chromodynamics (QCD). Predictions derived from perturbative QCD, valid only at the parton level, are, at present, still quite crude. The quark and gluon multiplicity in a parton shower is an inherently infra-red unstable measure and, therefore, very sensitive to high-order contributions in α_s, the strong coupling constant.

The first analytical description of MD's in parton cascades, and in full phase space, goes back to the Leading Log Approximation (LLA) [10]. It turned out that the LLA is inadequate to describe the experimentally measured moments of the MD in e^+e^- annihilations. Improved results were obtained in the Double Leading Log Approximation (DLA) where the strong angular ordering prescription is used to account for destructive interference of soft gluons [11]. A noteworthy result of the DLA is the prediction of KNO-scaling for the MD of gluons in a gluon jet.

In 1972, Koba, Nielsen and Olesen (KNO) [12] derived the asymptotic result, assuming Feynman-scaling [13], that the product of the average multiplicity $\langle n\rangle$ and the probability P_n for n charged particles in the final state is an energy-independent function $\Psi(z) = \langle n\rangle\, P_n$ with $z \equiv n/\langle n\rangle$. If P_n obeys KNO-scaling, then the dispersion $D = \sqrt{\langle n^2\rangle - \langle n\rangle^2}$ is proportional to $\langle n\rangle$.

The asymptotic value of $\langle n\rangle/D$ is, in DLA, predicted to be $\sqrt{3}$. In addition, the function $\Psi(z)$ turns out to be independent of α_s, a result first noted in [14].

Approximate KNO-scaling is observed experimentally at present energies, e.g. in e^+e^- annihilations and lepton-hadron collisions, but the shape of the scaling function is very different from that computed in DLA, especially for large n. To take into account proper recoil kinematics (which implies at least one extra order in α_s) the Modified Leading Log Approximation (MLLA) was introduced. Calculations of MD's have recently been performed, both with running and with fixed coupling constant [15] (see also [6]). KNO-scaling is found to be valid only at extremely high energies. For large z, the function $\Psi(z)$ widens very slowly with energy with a rate determined by the multiplicity anomalous dimension. The latter governs the growth with energy of the average parton multiplicity in a jet. The predicted scaling function comes close to e^+e^- data at LEP energies for n well above $\langle n\rangle$ but fails dramatically for smaller n. The results of the MLLA calculations can in several respects be improved upon in the Lund colour-dipole model, discussed in [16].

Evidently, all perturbative QCD results are valid at the parton level only. To connect the predictions with the world of hadrons one may resort to phenomenological models of hadronisation, matching the initial parton cascading based on perturbative QCD. Such models provide excellent descriptions of the data, especially for e^+e^- annihilations. Alternatively, one may use concepts such as Local Parton Hadron Duality (LPHD) [17] to compare theoretical predictions with experimental data. LPHD, based on the idea of preconfinement, assumes a direct proportionality between *partonic* single-inclusive distributions and *hadronic* ones and has turned out to be surprisingly successful. As far as MD's are concerned, however, the LPHD hypothesis must be extended to all q-particle inclusive distributions ($q \geq 1$). Such an extension was proposed [18] and motivated by the observation that the multiplicity distribution of partons in parton showers can, to a good approximation, be described by Negative Binomial distributions (NBD) [19]. The generalized LPHD hypothesis ensures that the NBD-character of MD's is maintained at the hadron level.

Experimentally, it is indeed well-established that MD's, in full phase space as well as in restricted phase space domains, are approximately of Negative Binomial form in a large variety of collision processes, although deviations are expected, and observed [20], in final states comprising multiple jets.

The Negative Binomial distribution can be represented in the form

$$P(n;k,\overline{n}) = \frac{k(k+1)\cdots(k+n-1)}{n!}\left(\frac{\overline{n}}{\overline{n}+k}\right)^n \left(\frac{k}{\overline{n}+k}\right)^k, \tag{1}$$

with k (or $1/k$) and $\overline{n}$ as free parameters. The average multiplicity $\langle n\rangle$ and the dispersion D of the NBD are related to the two parameters by

$$\langle n\rangle = \overline{n} \text{ and } \frac{D^2}{\langle n\rangle^2} = \frac{1}{\langle n\rangle} + \frac{1}{k}. \tag{2}$$

For $1/k \to 0$ (eqn.1) reduces to a Poissonian.

In deep-inelastic lepton-hadron and lepton-nucleus collisions, the NBD has been used extensively and found to provide an adequate description of the MD's of negative or all-charged hadrons for full phase space, in limited (pseudo-)rapidity intervals, as well as in the full current (forward) and nucleon (backward) hemispheres defined relative to hadronic centre-of-mass frame [4,21]

In this paper, we analyse deep-inelastic e^+p data at HERA in terms of the Negative Binomial distribution for domains of the four-momentum squared ($q^2 = -Q^2$) transferred from the positron, and the invariant mass of the hadronic system W, inaccessible at previous accelerators. The average charged multiplicity $\langle n\rangle$ and the ratio $\langle n\rangle/D$, derived from NBD fits, are studied as functions of Q^2 and W in the current-fragmentation region of the hadronic centre-of-mass. The results are compared with lower-energy lepton-nucleon DIS experiments and with data on e^+e^- annihilations.

The paper is further organised as follows. In sections 2.1-2 we give details on the experiment and on event and track selection criteria. Section 2.3 contains a description of correction procedures used to measure the NBD parameters. A discussion of systematic errors affecting our measurements is given in Sect. 2.4. The experimental results are presented in Sect. 3. Finally, a summary of observations is given in Sect. 4.

2 Experimental procedure

2.1 The experiment

The experiment was carried out with the H1 detector [22] at the HERA storage ring in DESY. The data were collected during the 1994 running period when 27.6 GeV positrons collided with 820 GeV protons, at a centre-of-mass energy of 300 GeV.

2.2 Event and track selection

The analysis is based on charged particles only. These are measured by two cylindrical drift chambers (CJC), mounted concentrically around the beamline inside a homogeneous magnetic field of 1.15 Tesla, providing particle charge and momentum from track curvature.

A neutral current DIS event selection is made by demanding a well-reconstructed scattered positron of energy larger than 12 GeV. This eliminates most of the photoproduction background. Two samples were considered. The "low-Q^2" sample ($12 < Q^2 < 80$ GeV^2) consists of events in which the scattered positron is detected in the Backward Electromagnetic Calorimeter (BEMC). The events of the "high-Q^2" sample ($Q^2 > 100$ GeV^2) have a positron detected in the Liquid Argon calorimeter (LAr).

Various sources of background are further reduced by appropriate selections. To exclude events with large radiative effects and to ensure substantial hadronic energy flow in the detector, the invariant mass squared W^2 of the hadronic system, determined from energy clusters in the calorimeter, must be larger than 4400 GeV^2. The energy E_F deposited in the calorimeter in the forward (beam proton) direction within the polar angle range $4.4° < \theta < 15°$ has to be larger than 0.5 GeV, to remove diffractive ("rapidity-gap") [23] events.

Further cuts are applied to ensure a good quality reconstructed scattered positron, which is used to determine the event kinematics. An event vertex, reconstructed from tracks in the central tracker, within ± 30 cm of the mean vertex position, is required to reject beam-induced background and to ensure good determination of the kinematic variables. Events with coherent noise in the calorimeter or with a time of flight veto from the scintillator hodoscope are rejected.

The high-Q^2 sample is subjected to additional quality selections. Cuts are applied to reject halo muons and to ensure p_T balance. Photoproduction background is further reduced by demanding the Bjorken scaling variable y to be less than 0.6.

Charged particle tracks are selected using CJC information only. Tracks must have a polar angle in the range 22° and 150°. The lower value is to ensure a good track finding efficiency, the upper cut is mainly applied to exclude the positron track in the low-Q^2 sample. In the high-Q^2 sample the positron track is identified with a track-cluster linking algorithm. In addition, the transverse momentum of a track must be larger than 0.15 GeV/c and the track must be linked to the primary event vertex. When applying these selection criteria the reconstruction efficiency is larger than 95 %.

A total of 73515 low-Q^2 and 3175 high-Q^2 events satisfied the above selection criteria, corresponding to an integrated luminosity of 1.3 pb^{-1}.

2.3 Simulation and unfolding procedure

The multiplicity distribution of charged hadrons observed in the experiment needs to be corrected for many effects. The geometrical acceptance of the central tracking device is limited and changes from event to event due to the Lorentz boost to the hadronic center-of-mass system. Furthermore, corrections have to be applied for the limited efficiency of track finding, particle interactions in the detector material and other detector imperfections. Background from radiative events and events that migrated into the kinematical bin considered, has to be accounted for. Also the effect of event loss due to event selection or kinematical migration out of the bin considered, has to be taken into account. Finally, the MD has to be corrected for contributions from decay products of K^0_S, Λ and $\overline{\Lambda}$.

To calculate the true number of events $M^{all}(m)$ with true multiplicity m of charged hadrons in an event using the actually observed number of events $N^{obs}(n)$ with observed multiplicity n, a statistical unfolding method is needed. In the majority of previous studies this is accomplished via migration-matrix techniques [24–27], based on full Monte Carlo simulation of the detector response[1].

For the analysis presented here, we have adopted a method (cfr. [21]) whereby the observed multiplicity distributions are not directly corrected. Instead, a theoretical distribution $M^{all}_{T(\vec{a})}(m)$, with parameters $\vec{a}$, is transformed into a reconstructed distribution whereby all detector effects are taken into account. The function $M^{all}_{T(\vec{a})}(m)$ represents the true multiplicity distribution for ideal non-radiative deep-inelastic collisions. The transformed ("smeared") distribution $N^{obs}_{T(\vec{a})}(n)$ is then compared to the measured one and the parameters $\vec{a}$ determined from a minimum-χ^2 procedure. For the theoretical distribution we have chosen the Negative Binomial distribution with parameters $\overline{n}$ and $1/k$.

The method used has several advantages, but also several shortcomings. Advantages are that the migration matrix is readily determined and is independent of the multiplicity distribution of the model used in the Monte Carlo simulation. It depends strongly, however, on the detector response, as required. Moreover, fits can be performed using the actually observed, and essentially uncorrelated, frequencies for each charged particle multiplicity.

Disadvantages are i) that a fully corrected multiplicity distribution is not obtained but only a set of moments, ii) the input distribution is imposed apriori.

The necessary information to do this smearing is obtained form a Monte Carlo simulation program. Neutral current DIS events were generated using the HERACLES program [28] which incoporates first-order electroweak corrections. The Monte Carlo generator LEPTO [29], interfaced to HERACLES via the program DJANGO [30], was used to simulate QCD cascades and fragmentation. The parton cascade was modelled with the colour-dipole model, using the ARIADNE [31] program. To study systematic effects another sample of Monte Carlo event was generated using the matrix element plus parton shower option (MEPS) within LEPTO. These models use the Lund string fragmentation model [32] for the hadronisation phase as implemented in JETSET [33].

The detector simulation program is based on the GEANT [34] program. Finally the generated and simulated events go through the same reconstruction and analysis chain as

[1]In parallel with the analysis presented here, we have used several matrix-unfolding methods as a cross-check of the results of this paper. Detailed results will be published elsewhere

the real data events.

The smearing was applied as follows. First the input NBD at fixed multiplicity m is reduced to take into account the loss of events.

$$M^{obs}_{NBD}(m) = M^{all}_{NBD}(m)\frac{M^{obs}_{mc}(m)}{M^{all}_{mc}(m)} \tag{3}$$

Here $M^{all}_{NBD}(m)$ is the input NBD for all events, while $M^{obs}_{NBD}(m)$ is the input NBD for observed events only. Similar definitions are used for Monte Carlo.

In the next step the migration in multiplicity is taken into account. A migration matrix $\mathcal{M}^{obs}_{mc}(m,n)$ is obtained from Monte Carlo. The matrix element (m,n) is equal to the observed number of events with generated multiplicity m and observed multiplicity n. The smeared NBD is equal to

$$N^{obs}_{NBD}(n) = \sum_m M^{obs}_{NBD}(m)\frac{\mathcal{M}^{obs}_{mc}(m,n)}{M^{obs}_{mc}(m)} \tag{4}$$

Finally radiative effects and migration of kinematical variables into the bin considered is accounted for. This background $N^{obs}_{back}(n)$ is estimated from the Monte Carlo simulation. The final smeared NBD that will be fitted to the observed data multiplicity is now equal to

$$N^{obs}_{NBD+back}(n) = N^{obs}_{NBD}(n) + N^{obs}_{NBD}\frac{N^{obs}_{back}(n)}{N^{obs}_{mc}}, \tag{5}$$

where $N^{obs}_{NBD} = \sum_n N^{obs}_{NBD}(n)$ and $N^{obs}_{mc} = \sum_n N^{obs}_{mc}(n)$ are the total number of observed events from the NBD and the Monte Carlo respectively.

The fit is performed by minimizing a χ^2 defined as follows :

$$\chi^2 = \sum_n \frac{(N^{obs}_{NBD+back}(n) - N^{obs}_{data+back}(n))^2}{\delta N^{obs}_{NBD+back}(n)^2 + \delta N^{obs}_{data+back}(n)^2} \tag{6}$$

It is important to note that $\delta N^{obs}_{NBD+back}(n)$ also depends on the fit parameters $\overline{n}$ and $1/k$. The error of the smeared NBD is due to the limited Monte Carlo statistics.

2.4 Systematic errors

To study systematic effects several checks were performed. The most important possible sources of systematic errors are i) residual background events, ii) event and track selection cuts and iii) the Monte Carlo generator used to smear the Negative Binomial Distribution.

The largest systematic error is due to the influence of the Monte Carlo generator. Although the smearing method is not explicitly dependent on the input multiplicity distribution, the detector simulation will be dependent on the generated topology of the events and so will be the migration matrix that is used in the smearing. The background subtraction and the estimation of lost events are, of course, also influenced by the Monte Carlo generator. Different Monte Carlo generators were used to estimate the systematic error. A 50 % error was taken on the large acceptance correction needed for the full hemisphere data points. To take into account the uncertainty of the track reconstruction efficiency estimated from Monte Carlo a 5 % systematic error is used. This results in a 12 % error on $\langle n_{ch} \rangle$ and 8 % error on $\langle n_{ch} \rangle / D$. The error on $\langle n_{ch} \rangle$ in the rapidity interval $1 < \eta^* < 5$ is 6 %.

The event selection criteria suppress background from photoproduction and radiative events. Although the Monte Carlo generator includes radiative effects, the possible remaining background was taken into account by relaxing the event selection. Other general event quality cuts were also altered. The overall systematic error due to the event selection was found to be 3 % and 6% on $< n_{ch} >$ and $< n_{ch} > / D$ respectively.

Finally, the track selection cuts were changed. Cuts on θ and p_T were removed, so that tracks from less efficient regions of the central tracker were also allowed to enter the observed multiplicity distribution. This causes significant changes in the migration matrix, but affects the values of the fitted parameters by less than 1 %.

3 Results

The multiplicity distribution was studied in 16 kinematical intervals in W and Q^2. Fig. 1 shows the observed multiplicity distribution (full circles) and the smeared NBD (open circles) for (upper figure) the full current hemisphere in the hadronic CMS and (lower figure) the pseudo-rapidity interval $1 < \eta^* < 5$ for which the detector acceptance is everywhere larger than 50% with an average of 80 %. The indicated errors are statistical only. The theoretical NBD (drawn as a continuous line for clarity) is represented by the solid lines. In all cases we find that the smeared NBD describes the raw data quite well. This suggests that the multiplicity distributions are approximately of NBD type and conforms with similar observations at much lower energy [27, 21].

In the fits, the data point $n = 0$ (no observed tracks in the considered pseudorapidity interval) was not included. There is a systematic discrepancy between data and the smeared NBD for the zero-multiplicity events that is problably due to remaining radiative events, not well accounted for in the Monte Carlo. Such events have an incoming positron with reduced momentum so that the hadronic system as a whole is shifted to the forward region (out of the Central Tracker) in the laboratory system.

Previous studies [35] have reported a significant variation with Q^2 or x of the hadron multiplicities in DIS μp scattering for fixed W. Analysis of the shape of the fragmentation function[2] $D^h(z_h)$ indicated that the increase of the particle yield with Q^2 takes place for low z_h particles. In the current fragmentation region ($z_h > 0.15$), a decrease in multiplicity with Q^2 was observed. Such effects are expected in QCD. In $\nu(\overline{\nu})N$ scattering, the average charged multiplicity is rather independent of Q^2 in fixed intervals of W [36].

Our data on $\langle n_{ch} \rangle$ are shown in Fig. 2 for four intervals of W. Within statistical and systematic errors, no significant dependence on Q^2 is observed. The straight lines are fits to a constant.

To study the W-dependence of $\langle n_{ch} \rangle$ and $\langle n_{ch} \rangle / D$, presented in Fig. 3, we have combined all Q^2-intervals and repeated the NBD fitting procedure.

The results for $\langle n_{ch} \rangle$ are plotted in Fig. 3a with statistical and systematic errors added in quadrature. For $\eta^* > 0$ as well as for $1 < \eta^* < 5$, $\langle n_{ch} \rangle$ varies linearly with $\ln W$ over

[2] z_h is the fraction of the total laboratory energy of the virtual boson carried by a hadron

the range covered by HERA. However, compared with DIS data at lower energy, it is evident that $\langle n_{ch} \rangle$ rises faster than linearly with $\ln W$. A fit with the form

$$\langle n_{ch} \rangle = a + b \ln W^2/\mathrm{GeV}^2 + c \ln^2 W^2/\mathrm{GeV}^2, \tag{7}$$

performed to the EMC [27], E665 [21][3] and the present data[4] yields $a = 1.79 \pm 0.21$, $b = -0.177 \pm 0.078$ and $c = 0.1069 \pm 0.0082$ with $\chi^2 = 86.3$ for 18 degrees of freedom. The large χ^2 of the fit is related to the systematic difference between the EMC and E665 results, and is discussed in [21]. This notwithstanding, the HERA data allow to confirm, for the first time in DIS lepton-nucleon scattering, the faster-than-linear growth with W of the average charged particle multiplicity in the current fragmentation region, already well-documented in e^+e^--annihilations and in hadron-hadron collisions.

For further comparison, we have included in Fig. 3a representative single-hemisphere e^+e^- results (corrected for K^0_S, Λ and $\overline{\Lambda}$ decays) at LEP [25], KEK [37] and PETRA [24] energies. These data follow quite closely the W-dependence of the DIS data.

A noteworthy disagreement is seen with the predictions of the DJANGO (dashed) and MEPS (dotted) Monte Carlo models which fall significantly below the data, also for $1 < \eta^* < 5$ (lower curves).

Finally, to study scaling of the multiplicity distribution we present in Fig. 3b the ratio $\langle n_{ch} \rangle / D$ as function of W, together with lower-W DIS data and e^+e^- results. Apart from a possible rise below 10 GeV, no evidence is seen for any significant change of this ratio over the energy-range from 10 to 200 GeV. This result provides a first indication that KNO-scaling remains valid up to HERA-energies. However, to draw firmer conclusions on KNO-scaling and related phenomena, it is necessary to study the energy dependence of the higher-order moments, and, therefore, the full multiplicity distribution.

4 Summary

The charged particle multiplicity distribution has been studied in DIS e^+p collisions with the H1 detector. A migration- matrix technique is used, based on multiplicity distributions of Negative Binomial type, to measure the average charged hadron multiplicity $\langle n_{ch} \rangle$ and the ratio $\langle n_{ch} \rangle / D$ in intervals of Q^2 and W in the hadronic CMS current fragmentation region.

No evidence is found for a significant Q^2-dependence, at fixed W, of $\langle n_{ch} \rangle$. The average charged hadron multiplicity exhibits a faster-than-linear rise with $\ln W$, compatible with that earlier observed in e^+e^- annihilation data and hadron-hadron collisions. This behaviour is predicted in perturbative QCD. The near energy-independence of $\langle n_{ch} \rangle / D$ suggests that KNO-scaling may remain valid in DIS processes in the range of energies from 10 to 200 GeV.

[3] In the E665 data sample, events due to diffractive ρ^0 production are excluded

[4] We checked that including "rapidity-gap" events changes $\langle n_{ch} \rangle$ by less than the systematic error

Acknowledgements

We are grateful to the HERA machine group whose outstandig efforts made this experiment possible. We thank the engineers and technicians for their work in constructing and now maintaining the H1 detector, our funding agencies for financial support, the DESY technical staff for continual assistance, and the DESY directorate for the hospitality they extend to the non-DESY members of the collaboration.

References

[1] H1 Coll., S. Aid *et al., A study of the fragmentation of quarks in e^-p collisions at HERA*, DESY preprint DESY 95-072 (1995).

[2] ZEUS Coll., M. Derrick *et al., Measurement of multiplicity and momentum spectra in the current fragmentation region of the Breit frame at HERA*, DESY preprint DESY 95-007 (1995).

[3] *Multiparticle Dynamics* (Festschrift L. Van Hove), Eds. A. Giovannini and W.Kittel (World Scientific, Singapore 1990);
G. Giacomelli, Int. J. Mod. Phys. **A5** (1990) 223.

[4] For comprehensive reviews see N. Schmitz, Int. J. Mod. Phys. **A3** (1988) 1997;
Int. J. Mod. Phys. **A8** (1993) 1993.

[5] P. Carruthers and C.C. Shih, Int. J. Mod. Phys. **A2** (1987) 1147.

[6] I.M. Dremin, *Quantum Chromodynamics and Multiplicity Distributions* Physics-Uspekhi **37** (1994) 4077; hep-ph-9406231.

[7] R. Ugoccioni, *Multiplicity Distributions* in Proc. XXIV Int. Symp. on Multiparticle Dynamics, Vietri-sul-Mare, Italy, 1994, Eds. A. Giovannini, S. Lupia, R.Ugoccioni (World Scientific, Singapore 1995) p.384.

[8] W. Heisenberg, Z.Phys. **113** (1939) 61; Nature (London) **164** (1949) 65.

[9] E. Fermi, Prog. Theor. Phys. **5** (1950) 570.

[10] K. Konishi, A. Ukawa, G. Veneziano, Nucl. Phys. **B157** (1979) 45.

[11] Yu.L. Dokshitzer, V.A. Khoze, A.H. Mueller, S.I. Troyan, *Basics of Perturbative QCD*, Edition Frontières, Gif-sur-Yvette, 1991.

[12] Z.Koba, H.B. Nielsen and P. Olesen, Nucl. Phys. **B40** (1972) 317.

[13] R.P. Feynman, Phys. Rev. Lett. **23** (1969) 1415.

[14] A. Basetto, M. Ciafaloni, G. Marchesini, Nucl. Phys. **B163** (1980) 477.

[15] Yu.L. Dokshitzer, Phys. Lett. **B305** (1993) 295.

[16] G. Gustafson, Nucl. Phys. **B392** (1993) 251;
G. Gustafson, M. Olsson, Nucl. Phys. **B406** (1993) 293.

[17] D. Amati, G. Veneziano, Phys. Lett. **B83** (1979) 87;
G. Marchesini, L. Trentadue, G. Veneziano, Nucl. Phys. **B181** (1981) 335;
Ya.I. Azimov, Yu.L. Doskshitzer, V.A. Khoze, S.I. Troyan, Z. Physik C–Particles and Fields **C27** ((1985) 65, Z. Physik C–Particles and Fields **C31** (1986) 213.

[18] L. Van Hove, A. Giovannini, Acta. Phys. Pol. **B19** (1988) 917.

[19] A. Giovannini, L. Van Hove, Z. Physik C–Particles and Fields **C30** (1986) 391.

[20] P. Abreu et al. (DELPHI) Z. Physik C–Particles and Fields **C52** (1991) 271; Z. Physik C–Particles and Fields **C56** (1992) 63.

[21] E665 Coll., M.R. Adams *et al.,* Z. Physik C–Particles and Fields **C61** (1994) 179.

[22] H1 Coll., I. Abt *et al., The H1 detector at HERA* DESY preprint DESY 93-103 (1993).

[23] H1 Coll., T. Ahmed *et al.,* Nucl. Phys. **B249** (1994) 477.

[24] TASSO Coll., W. Braunschweig *et al.,* Z. Physik C–Particles and Fields **C45** (1989) 193.

[25] DELPHI Coll., P. Abreu *et al.,* Z. Physik C–Particles and Fields **C50** (1991) 185.

[26] OPAL Coll., P.D. Acton *et al.,* Z. Physik C–Particles and Fields **C53** (1992) 539.

[27] European Muon Coll., M. Arneodo *et al.,* Z. Physik C–Particles and Fields **C35** (1987) 335.

[28] A. Kwiatkowski, H. Spiesberger and H.-J. Möhring, Proceedings of the 1991 Workshop on Physics at HERA, DESY Vol.3 (1992) 1294.

[29] G. Ingelman, Proceedings of the 1991 Workshop on Physics at HERA, DESY Vol.3 (1992) 1366.

[30] K. Charchula, G. Schuler and H. Spiesberger, CERN-TH.7133/94.

[31] L. Lönnblad, Comp. Phys. Comm. **71** (1992) 15.

[32] B. Andersson *et al.,* Phys. Rep. **97** (1983) 31.

[33] T. Sjöstrand, Comp. Phys. Comm. **39** (1986) 346;
T. Sjöstrand and M. Bengtsson, ibid. 43 (1987) 367.

[34] R. Brun *et al.,* GEANT3, CERN DD/EE/84-1 (1987).

[35] M. Arneodo *et al.,* Z. Physik C–Particles and Fields **C31** (1986) 1; Phys. Lett. **B165** (1985) 222.

[36] H. Grässler *et al.,* Nucl. Phys. **B233** (1983) 269;
B. Barlag *et al.,* Z. Physik C–Particles and Fields **C11** (1982) 283, **C14** (1982) 281, erratum.

[37] H.W. Zheng *et al.,* Phys. Rev. **D42** (1990) 737.

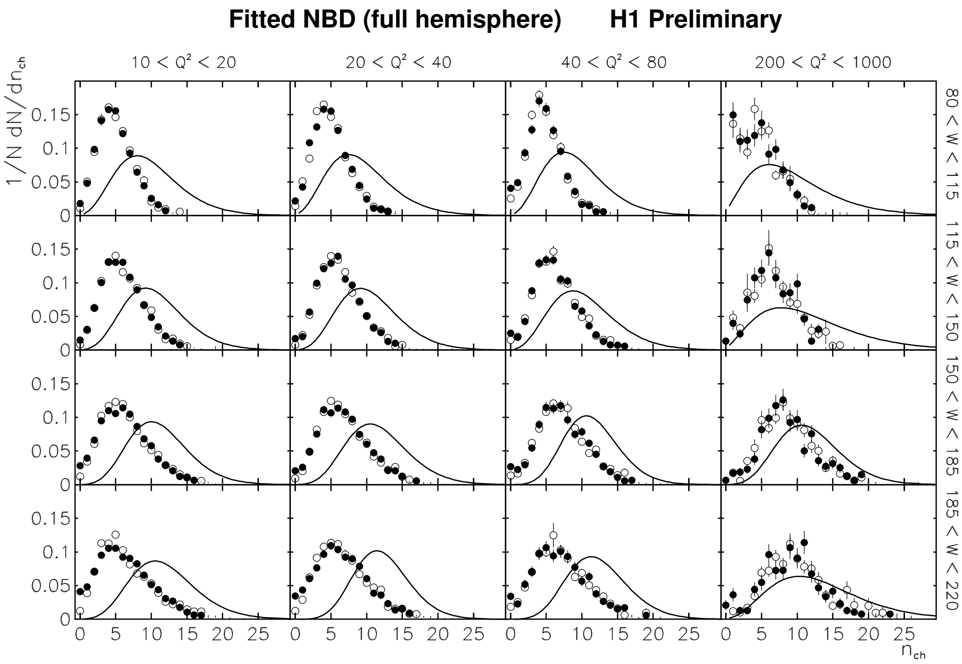

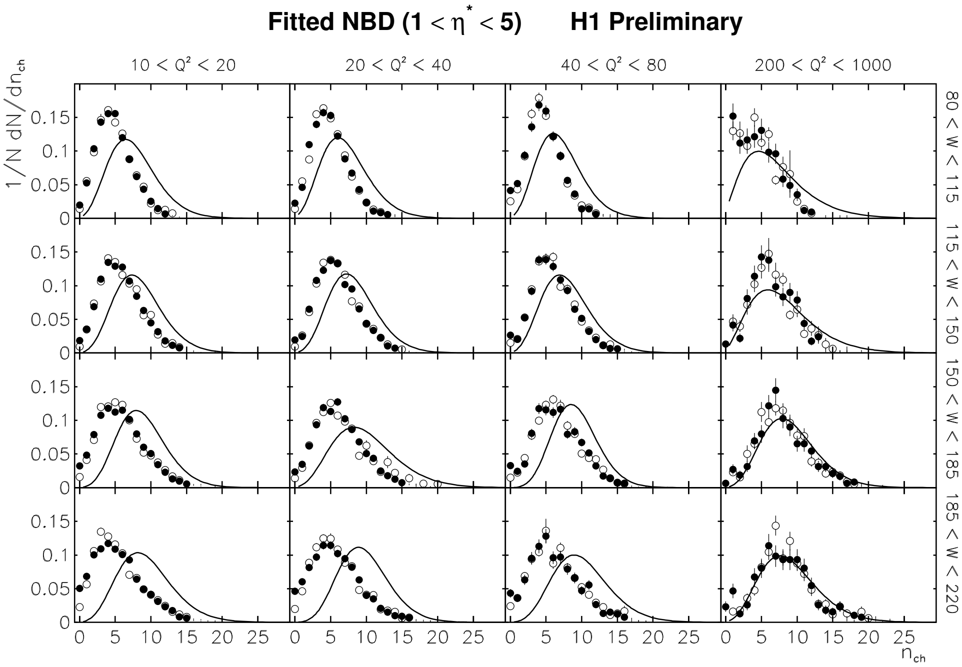

Figure 1(a-b) : The NBD (line) is smeared to an observed distribution (open circles). The latter is fitted to the observed data points (full circles) in 16 bins in W (GeV) and $Q^2(\mathrm{GeV}^2)$. The first point (zero multiplicity) is not included in the fit. The top figure shows MDs for the full current hemisphere, while in the lower figure tracks are restricted to a range in pseudorapidity η^*.

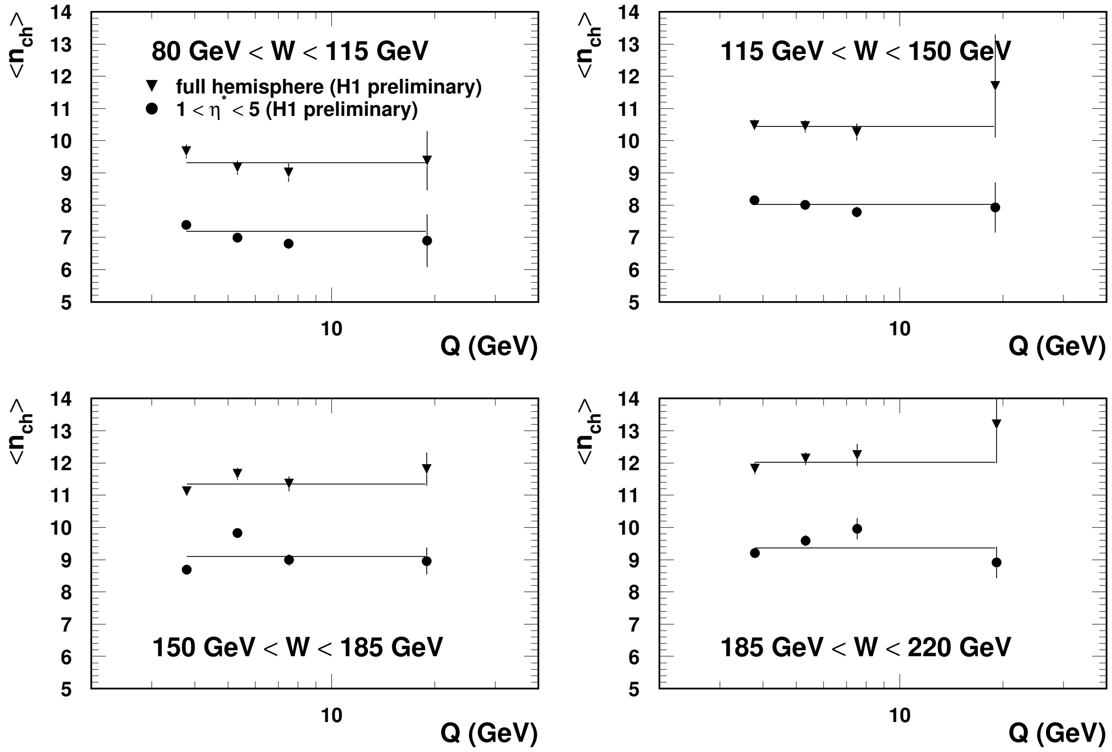

Figure 2 : $\sqrt{Q^2}$ dependence of the average charged hadron multiplicity in intervals of W and pseudorapidity η^*. The data show no significant dependence on Q^2. Horizontal lines are fits to a constant. Error bars show statistical errors only.

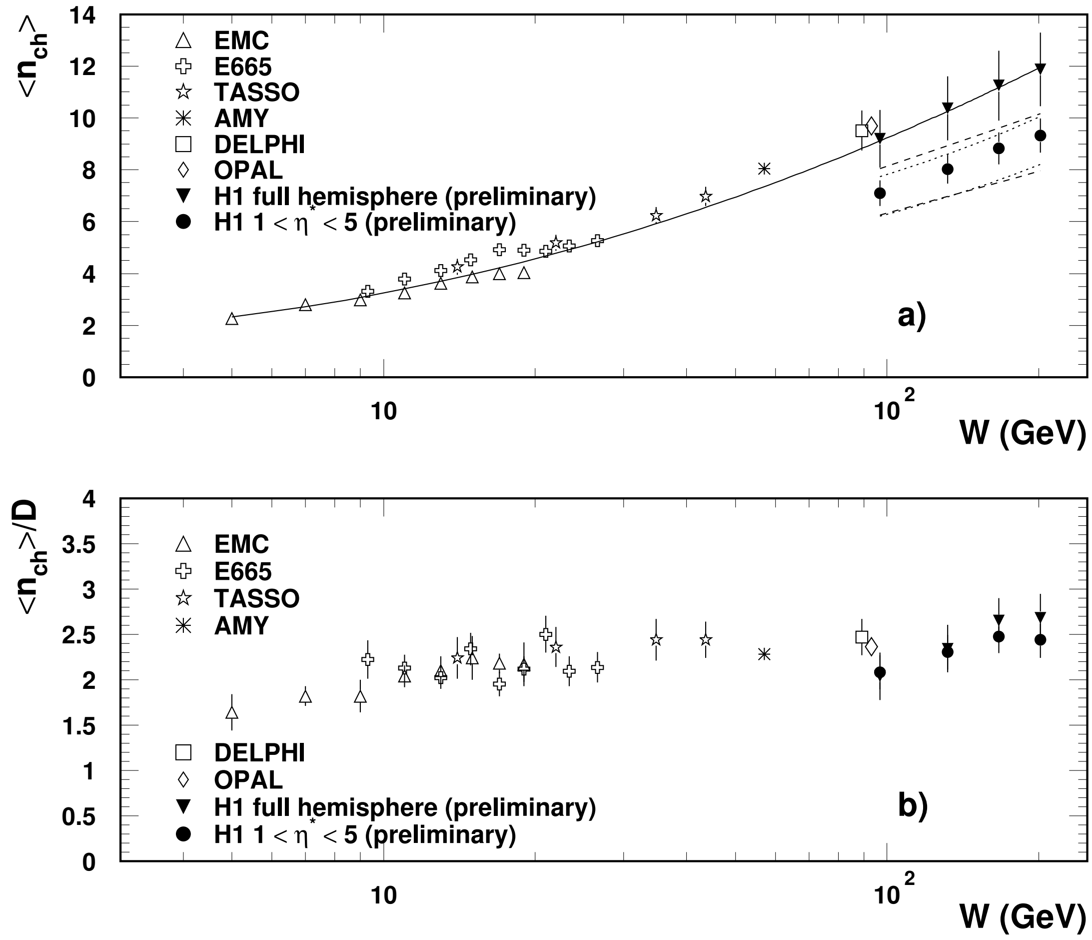

Figure 3 : The top figure (**a**) shows the W dependence of the mean multiplicity. H1 preliminary data points are compared to other experiments. Systematic errors are included in the error bars. The solid line shows a fit of the form $\langle n_{ch}\rangle = a + b\ln W^2 + c\ln^2 W^2$ to the data points of DIS experiments (EMC, E665 and H1). The dashed (dotted) line shows the prediction of the DJANGO (MEPS) Monte Carlo program, which is significantly lower for both ranges in pseudorapidity. In the lower figure (**b**) $\langle n_{ch}\rangle/D$ is plotted as a function of W as an indication for KNO-scaling.